Available online at www.sciencedirect.com
ScienceDirect
J. of Supercritical Fluids 44 (2008) 193–200
THE JOURNAL OF Supercritical Fluids
www.elsevier.com/locate/supflu

# Characterization of high-pressure carbon dioxide explosion to enhance oil extraction from canola

Meidui Dong, Terry H. Walker *

*Biosystems Engineering, Clemson University, Biosystems Research Complex, 51 New Cherry Street, Clemson, SC 29634, USA*

Received 9 August 2007; received in revised form 20 October 2007; accepted 27 October 2007

**Abstract**

The change of pressure, temperature and phase during high-pressure carbon dioxide explosion process were investigated. Different initial temperature and pressure conditions were chosen, ranging from 25 to 65 °C and 500 to 3000 psi covering initial liquid, supercritical and gas phases. Under certain initial conditions with low temperature and high pressure, the depressurization process caused a phase change that increased the release time where the depressurization–time curves did not exponentially decrease. This explosion process was characterized based on total release time, rate of depressurization, and effect of phase change on the rate of depressurization. The temperature change associated with the change of pressure was also discussed. Canola flakes were exploded using chosen initial conditions. Oil extraction from canola flakes using supercritical carbon dioxide was improved after explosion treatment. Explosion at 35 °C and 3000 psi of initial condition resulted in the highest oil yield.


*Keywords:* Characterization; High-pressure carbon dioxide; Explosion; Supercritical fluid extraction; Canola oil

## 1. Introduction

High-pressure carbon dioxide explosion is a process of rapid release of pressurized carbon dioxide by quickly opening an exit valve. Different names of similar processes were used in published literature, such as explosive depressurization, rapid depressurization, explosive decompression, flash decompression, flash discharge, blowdown, etc. The process of rapid depressurization of a gas storage cylinder or vessel through an orifice or nozzle was theoretically and experimentally studied using air, hydrogen and nitrogen as model gases in early work [1–3]. These works concentrated on modeling and experimental comparison of fluid thermodynamic processes for pressure–time and temperature–time changes.

The explosion process was developed for some chemical and biological applications to treat the sample in a high-pressure vessel. For example, explosion processes were investigated for sterilization [4–6], activation and denaturation of enzyme [7,8], and pretreatment of lignocellulosic substrates [9,10]. The mechanisms for these applications involve mechanical cell rupture, chemical and biochemical modification of the structure of treated sample and their synergistic effects, utilizing several advantages of high-pressure carbon dioxide. The processes of rapid or flash depressurization were not quantitatively characterized for how the depressurization was progressing rapidly with time and for the effect on the treated sample in small volume vessels. However, the characterization for this dynamic process of rapid depressurization is important either to understand the mechanism or to direct further experimental design and analysis. Also, the phase behavior transition with the decrease of pressure and temperature during decompression may considerably affect the physical characteristics of treated samples.

To better understand the process of high-pressure explosion and its application for biological processing, the change of pressure and phase within a high-pressure vessel during the explosion process were investigated for carbon dioxide in this study. Initial temperature and pressure conditions were chosen to encompass initial liquid, supercritical and gas phases. Canola flake was investigated as a biological model system for the effect on extractability of canola oil using supercritical carbon dioxide after the explosion pretreatment.

## 2. Experimental equipment and methods

### 2.1. Experimental equipment

Fig. 1 shows the explosion apparatus, which consisted of five major components: syringe pump (ISCO, USA), high-pressure

* Corresponding author. Tel.: +1 864 656 0351; fax: +1 864 656 0351.
*E-mail address:* walker4@clemson.edu (T.H. Walker).

0896-8446/$ – see front matter © 2007 Elsevier B.V. All rights reserved.
doi:10.1016/j.supflu.2007.10.010

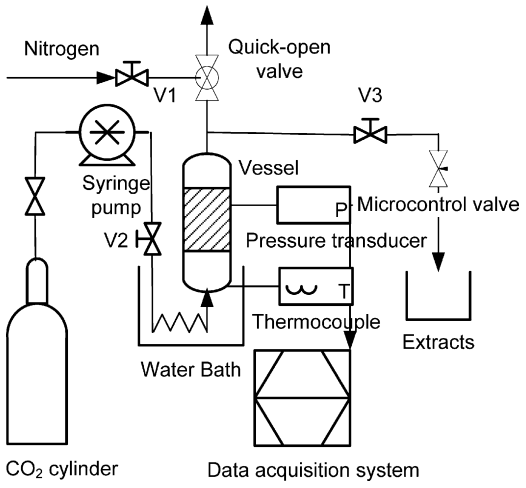


Fig. 1. Schematic diagram of the explosion and extraction apparatus.

vessel (Thar Design, USA), quick-open ball-valve (Swagelok, SS-83KS4-31C, USA), temperature-controlled water bath and data acquisition system. Omega flow meter (Omega Engineering, FMA-2305, USA) was used to measure flow rate of effluent $CO_2$ gas at atmospheric conditions. This apparatus could be used for explosion, extraction or extraction following explosion. The system was set for explosion if valve V3 was closed and for extraction if kept open. The quick-open valve pneumatically actuated by 100 psi nitrogen gas was mounted to rapidly release the pressure inside the vessel.

A computerized data acquisition system for rapid collection of pressure and time data was developed for this apparatus. The data acquisition board (PCI-DAS08) was purchased from Measurement Computing Corporation, USA. The system software was programmed using Visual Basic. The sampling frequency of the PX-305 pressure transducer (Omega Engineering, PX-305, USA) could be set in the range from 5 to 100 kHz. The data were automatically saved to a spreadsheet file in Microsoft Excel.

### 2.2. Method for explosion process

Once all tubing connections were secured and the pneumatically actuated ball-valve was closed, the vessel was pressurized with $CO_2$ from the syringe pump until the experimental set pressure was achieved and held for 30 min to allow $CO_2$ and sample (if for treatment of sample) to reach the set experimental temperature. Then the valve between the vessel and pump was closed preventing gas exchange during the depressurization process. The data sampling frequency and duration were set with the software. Finally a rapid pressure release from saturation pressure to atmospheric pressure was imposed by opening the valve to activate the pneumatically actuated ball-valve using 100 psi nitrogen. Data were acquired at a sampling frequency of 500 Hz and duration of 10 s to characterize the rate of pressure decrease within the vessel.

A 75-ml vessel was coupled with frits at both ends to evenly distribute the fluid and to prevent treated sample from exiting the vessel. The explosions were compared, with or without frit and with or without canola flake sample. The canola flake was donated from Archer Daniels Midland Company (ADM, USA). Canola flake was the product of raw canola seed after the processing of preheating, flaking and cooking in the crushing plant. Prior to experiments, canola flake were stored at −20 °C for approximately 8 months. The flake particle size ranged from 1 to 2 mm and had a moisture content of 4% wet weight. Canola flake (10 g) was loaded in the vessel for each run. Three tests were conducted, without frit and canola sample (Case A), with frit and without canola sample (Case B) and with frit and canola sample (Case C). After the explosion process, the canola was frozen at −20 °C overnight before supercritical $CO_2$ extraction.

Explosions were carried out in each test, under five different initial temperatures, 25, 35, 45, 55 and 65 °C, at the same initial pressure of 1500 psi. Explosions were also conducted at four different initial pressures, 500, 1000, 1500 and 3000 psi at the same initial temperature of 35 °C.

### 2.3. Method for supercritical $CO_2$ extraction

Exploded canola flake (10 g) for Case C was loaded into the vessel. The vessel was pressurized to 5000 psi, and the bath temperature was set to 50 °C. After 30 min equilibration time, valve V3 and the micro-control valve were opened to produce a flow rate of approximately 700 ml/min. Unexploded canola flake was considered the experimental control and extracted under the same condition, 5000 psi, 50 °C and 700 ml/min flow rate. The extracted oil was trapped by glass beads in a 50-ml tarred centrifuge tube and weighed after 30 min, 1 h, and on the hour for a total extraction time of 7 h. To address the potential loss of oil during the explosion process, a mass balance determined that the amount of oil co-extracted during explosion was considered negligible at less than 0.4% of the total oil.

For modified extraction, 10 g canola flake was extracted for 3 h under the same extraction condition as above. After the internal pressure of vessel was slowly decreased to atmosphere, valve V3 was closed, and the flake was exploded by activating the quick-open valve under the same conditions as in Case C. After the quick-open valve was closed, the same extraction pressure of 5000 psi, temperature of 50 °C and flow rate of 700 ml/min were then set for another 3 h extraction. The extracted oil was trapped by glass beads in a 50-ml tarred centrifuge tube and weighed after each hour interval.

### 2.4. Oil composition analysis

Extracted oil was converted to fatty acid methyl esters (FAMEs) using a base-catalyzed transmethylation procedure [11]. Aliquots of about 5 mg sample were transferred to glass tubes. This aliquot was diluted with hexane to a volume of 0.5 ml. A mount of 20 μl of 1 M sodium methoxide in dry methanol and 20 μl of 1 M methyl acetate were added, then the mixture was vortexed and allowed to react for 5 min. The reaction was stopped by the addition of 4 μl of 1 M acetic acid. FAMEs were extracted by adding 1 ml of hexane, vortexing, centrifuging and transferring the hexane containing FAMEs to GC vial. FAMEs were analyzed using a HP6890 (Hewlett-Packard, San Fernando, CA) gas chromatograph equipped with

a HP7673A (Hewlett-Packard, San Fernando, CA) automatic sampler. Separation was accomplished using a 100-m SP2560 (Supelco, Bellefonte, PA) capillary column (0.25-mm i.d. and 0.20 μm film thickness). Column temperature was programmed to increase from 150 to 160 °C at 1 °C/min, from 160 to 167 °C at 0.2 °C/min, from 167 to 225 °C at 1.5 °C/min and held at 225 °C for 5 min. The injector and detector were maintained at 250 °C. Sample injection volume was 1 μl. Hydrogen was the carrier gas at a flow rate of 1 ml/min with a split ratio of 1:25. Peaks were identified by comparison to reference standards from Supelco (Bellefonte, PA). Fatty acids were quantified by incorporating a known amount of internal standard, heptadecanoic acid methyl ester (C17:0) (Nu-check prep Inc., USA) into each sample after methylation. Soxhlet extraction using hexane was employed for the canola feedstock to determine total oil by conducting the extraction until oil was completely depleted in the sample as determined by weight. Fisher Chemicals provided all reagents in this work unless otherwise noted.

### 2.5. Statistical analysis

Experimental data were subjected to analysis of least significant difference test (LSD) of multiple comparisons or Dunnett's test at 95% confidence ($\alpha = 0.05$) by Statistical Analysis System (SAS Ver. 9.1, SAS Institute, USA).

## 3. Results and discussion

### 3.1. Pressure–time history of explosion

The pressure–time curves for different initial pressures at 35 °C are shown in Fig. 2(a)–(c). Similar trends for Cases A–C were observed. At initial pressures of 500 and 1000 psi, the $CO_2$ was gaseous in the sub-critical phase. The depressurization curves are smooth, where the pressure decreased gradually within a short time of several seconds. At initial pressures of 1500 and 3000 psi, the $CO_2$ was in supercritical phase. The depressurization curves have two obvious sections, where pressure decreased quickly in the first section and less so in the later section. The point of rapid transition or abrupt break in the curve was determined by the inflection point or maximum change of depressurization rate. The data of total depressurization time, the pressure and time corresponding to the point of abrupt break are shown in Table 1. The presence of frit increased the depressurization time for Case B compared to Case A. For Case C, 10 g canola flake samples filled 25 ml of the total 75 ml vessel, and decreased the depressurization time due to reduced $CO_2$ volume. On the other hand, canola flake sample elongated the depressurization time due to its resistance. As a result, Case C had the longest pressure release time compared to Case A and Case B. The longest time was 9.620 s for case C at 3000 psi and the shortest total depressurization time was 0.728 s for case A at 500 psi.

The pressure–time curves under different temperatures at 1500 psi of initial pressure are shown in Fig. 3(a)–(c). Similar trends for Cases A–C were also observed. At initial temperatures of 55 and 65 °C, the depressurization curves were smooth. At initial temperatures of 25 and 35 °C, the depressurization curves again contained two distinctive sections. At an initial temperature of 45 °C, the depressurization curve transitioned without a distinctive break. The data of total depressurization time, the pressure and time corresponding to the point of abrupt break are shown in Table 2. The total depressurization time decreased with an increase of initial temperature in each case. This result was consistent with the viscosity behavior of supercritical fluids, which decreased with increasing temperature at the same pressure. Therefore, the fluids with lower viscosity depressurized more quickly. The frit and canola flake filling showed a similar effect on total depressurization time for each initial temperature. The longest depressurization time was >10 s for Case C at 25 °C and the shortest time was 1.168 s for Case A at 65 °C.

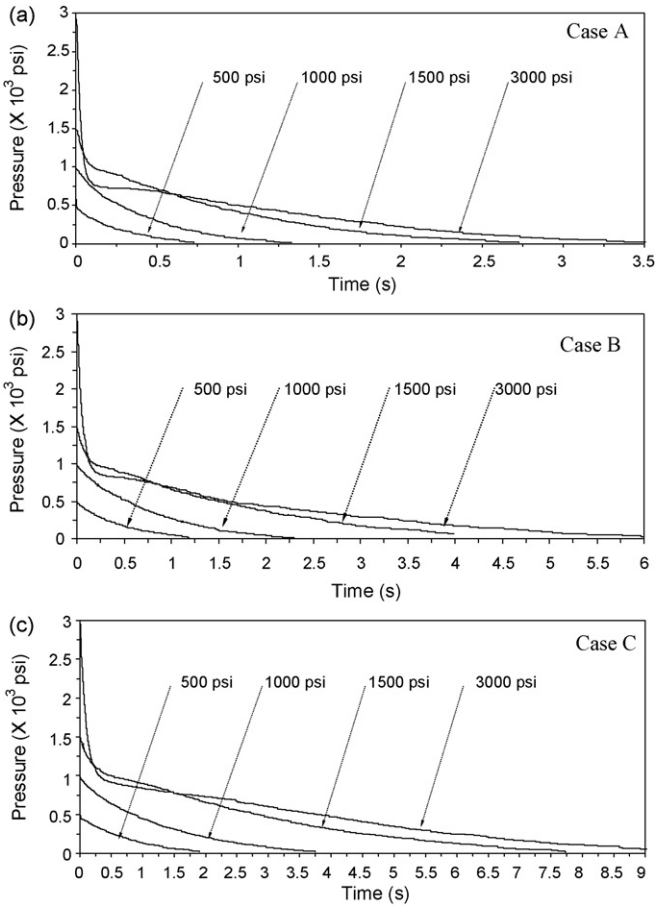


Fig. 2. Pressure–time trace of carbon dioxide subjected to different pressures for (a) Case A: without frit in place and canola sample; (b) Case B: with frit in place and without loading canola sample; (c) Case C: loaded with canola flake and frit in place. *Note*: Data was the average of two tests.

### 3.2. Comparison of the depressurization rate

The rate of depressurization, $\Delta P/\Delta t$, computed by corresponding data in Tables 1 and 2, is shown in Tables 3 and 4, respectively. The rate of depressurization increased with the increase of initial pressure or temperature within each case (see Figs. 2(a)–(c) and 3(a)–(c)). At each initial condition, the rate of depressurization decreases following Cases A–C. Again worthy

Table 1
Comparison of explosions under different pressures

| Initial pressure (psi) | Total time (s) Case | | | Phase change time (s) Case | | | Phase change pressure (psi) Case | | |
|---|---|---|---|---|---|---|---|---|---|
| | A | B | C | A | B | C | A | B | C |
| 500 | 0.728 | 1.182 | 1.908 | No abrupt change | | | No abrupt change | | |
| 1000 | 1.328 | 2.203 | 3.748 | | | | | | |
| 1500 | 2.728 | 4.078 | 7.730 | 0.150 | 0.247 | 0.476 | 949 | 969 | 1000 |
| 3000 | 3.502 | 5.999 | 9.620 | 0.090 | 0.184 | 0.364 | 818 | 909 | 970 |

*Note*: The data were total depressurization time, the pressure and time corresponding to the point of abrupt break shown in Fig. 2(a)–(c).

Table 2
Comparison of explosions under different temperatures

| Initial temperature (°C) | Total time (s) Case | | | Phase change time (s) Case | | | Phase change pressure (psi) Case | | |
|---|---|---|---|---|---|---|---|---|---|
| | A | B | C | A | B | C | A | B | C |
| 25 | 3.506 | 6.932 | >10 | 0.074 | 0.082 | 0.206 | 797 | 838 | 878 |
| 35 | 2.728 | 4.078 | 7.730 | 0.150 | 0.247 | 0.456 | 949 | 969 | 1000 |
| 45 | 1.658 | 2.610 | 4.608 | 0.182 | 0.318 | 0.536 | 909 | 919 | 980 |
| 55 | 1.282 | 2.226 | 4.018 | No abrupt change | | | No abrupt change | | |
| 65 | 1.168 | 2.122 | 3.300 | | | | | | |

*Note*: The data were total depressurization time, the pressure and time corresponding to the point of abrupt break shown in Fig. 3(a)–(c).

Table 3
Comparison of the rate of depressurization under different pressures

| Initial pressure (psi) | Rate of depressurization (psi/s) Case | | |
|---|---|---|---|
| | A | B | C |
| 500 | 687 | 423 | 262 |
| 1000 | 753 | 454 | 267 |
| 1500 | 550 [3693] (368) | 368 [2150] (252) | 194 [1050] (137) |
| 3000 | 857 [24244] (240) | 500 [11364] (156) | 312 [5577] (104) |

*Note*: The data were calculated according to $\Delta P/\Delta t$ from the data in Table 2. []: Rapid depressurization rate; (): lag depressurization rate.

of interest was the situations in which two-stage depressurization occurred. The total rate of depressurization was reduced at lower initial temperature in each case. The rates of depressurizations had two stages for the rapid and lag depressurization, compared to the smooth decompression. For example, for Case C in Table 3, the depressurization rate of rapid depressurization section of the curve was 5577 and 104 psi/s for lag section at 3000 psi initial pressure, compared to 267 psi/s of total depressurization rate for the initial pressure of 1000 psi (see Fig. 2(c)). This two-stage depressurization may affect the exploded sample differently depending on its variety and physical properties.

### 3.3. Discussion of experimental results

The explosion process may be treated ideally as an adiabatic expansion, which corresponds to an isenthalpic process. In the pressure–enthalpy diagram shown in Fig. 4, lines with arrows perpendicular to *X*-axis indicated the isenthalpic depressurization. At initial pressure and temperature corresponding to points 1, 2, 3 and 6, the depressurization curves cross the region where liquid and gas co-exist starting at the saturated liquid line or saturated gas line, which are indicated by points 1′, 2′, 3′ and 6′. The depressurization curves are not smooth, and the breaks occur at

Table 4
Comparison of the rate of depressurization under different temperatures

| Initial temperature (°C) | Rate of depressurization (psi/s) Case | | |
|---|---|---|---|
| | A | B | C |
| 25 | 482 [9500] (232) | 216 [8073] (122) | <150 [3019] (<90) |
| 35 | 550 [3673] (368) | 368 [2150] (253) | 194 [1096] (137) |
| 45 | 905 [3247] (615) | 575 [1827] (401) | 326 [970] (241) |
| 55 | 1170 | 674 | 373 |
| 65 | 1284 | 707 | 455 |

*Note*: The data were calculated according to $\Delta P/\Delta t$ from the data in Table 3. []: Rapid depressurization rate; (): lag depressurization rate.

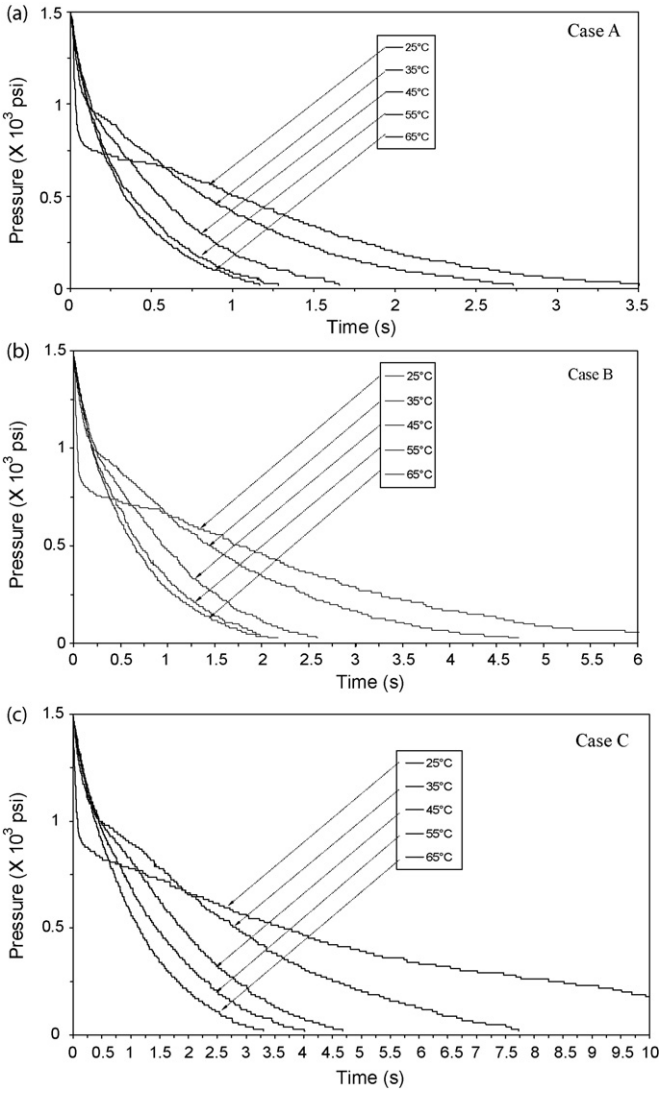


Fig. 3. Pressure–time trace of carbon dioxide subjected to different temperatures for (a) Case A: without frit in place and canola sample; (b) Case B: with frit in place and without loading canola sample; (c) Case C: loaded with canola flake and frit in place. *Note*: Data was the average of two tests.

points 1′, 2′, 3′ and 6′. The pressures at points 1′, 2′, 3′ and 6′ have the same trend as the values measured in the experiment shown in Tables 1 and 2 for each case, which increase following points 1′, 6′, 3′ and 2′. At initial pressures and temperatures corresponding to points 4, 5, 7 and 8, the depressurization curves do not cross the region where liquid and gas co-exist, so the curves are smooth and the transitions do not take place.

Furthermore, temperature inside the vessel decreases due to the expanding fluid associated with the change of pressure. As shown in Fig. 4, the isenthalpic depressurization line intersects the triple point, which enables the formation of dry ice. Higher initial pressure and lower initial temperature allow dry ice to form easier. The formation of dry ice will lengthen the time of pressure release. Byrnes et al. [1] investigated temperature and pressure change of hydrogen and nitrogen gasses by reducing pressure from 2000 to 200 psi. The hydrogen gas temperature dropped from 21.1 to −37.8 °C in 14 s decompression [1]. Defect ceramic material was formed in the supercritical $CO_2$ extraction process during depressurization. A temperature lower than −40 °C was detected at the end of depressurization. The stress from dry ice that formed within the ceramic body contributed more to the defect than that from the pressure gradient between the fluid of vessel and the porous body [12].

A rapid temperature drop to the freezing point may affect the viability of organisms or properties of matrix material. The mechanism of cell disruption by pressure gradient for the application of the explosion process was proposed and supported by X-ray and NMR examination [9] and by scanning electron microscopy [13]. To our understanding, another mechanism of cell disruption by cryogenic effect or synergistic effects of cryogenic and pressure gradients should be proposed. The extractability of essential oils from glandular trichomes treated by compressed $CO_2$ was similar to that treated by cryogenic comminution and better than ambient comminution [13]. A freezing process (e.g. cryogenic freezing, dry ice freezing and liquid nitrogen freezing) was patented for pretreatment of biomass to improve extractability [14]. Based on these finding, canola flake is a potential material that may be impacted by this freezing process.

### 3.4. Comparison of model with experimental data

A model for the pressure–time history in "blowing down" a pressured gas tank through a nozzle or an orifice was given under the isentropic and choked flow assumptions [1–3,15]. The thermodynamic properties of the gas in the vessel could be shown to obey isentropic relations by applying the integral continuity and energy equations to the control volume. For a large initial vessel pressure compared to the back pressure, the exit would be choked during most portions of the depressurization process.For the adiabatic case

$$\frac{P}{P_i} = \left[1 + \left(\frac{r-1}{2}\right)\left(\frac{r+1}{2}\right)^{-(r+1)/2(r-1)} \times \frac{t}{V/\left(A\sqrt{rRT_i}\right)}^{-2r/r-1}\right] \quad (1)$$

For the isothermal case

$$\frac{P}{P_i} = \exp\left[-\left(\frac{r+1}{2}\right)^{-(r+1)/2(r-1)} \frac{t}{V/\left(A\sqrt{rRT_i}\right)}\right] \quad (2)$$

where $P$ is pressure in the vessel; $P_i$, initial pressure in the vessel; $r$, gas specific heat ratio; $R$, gas constant; $t$, time; $V$, vessel volume; $A$, area of vessel exit; and $T_i$, initial temperature in the vessel. Gas specific heat ratio is the heat capacity at constant pressure over heat capacity at constant volume.

In this system, the vessel volume, $V$, is 75 ml. The area of vessel of valve exit, $A$, is 0.02 $cm^2$ with 1.6 mm diameter. The gas specific heat ratio for $CO_2$ is 1.3. For the different initial pressures at the same 35 °C of initial temperature, the theoretical and experimental results of the explosion process are shown in Fig. 5(a) and (b). For the 500 and 1000 psi initial pressures, the experimental results are between the adiabatic and isothermal

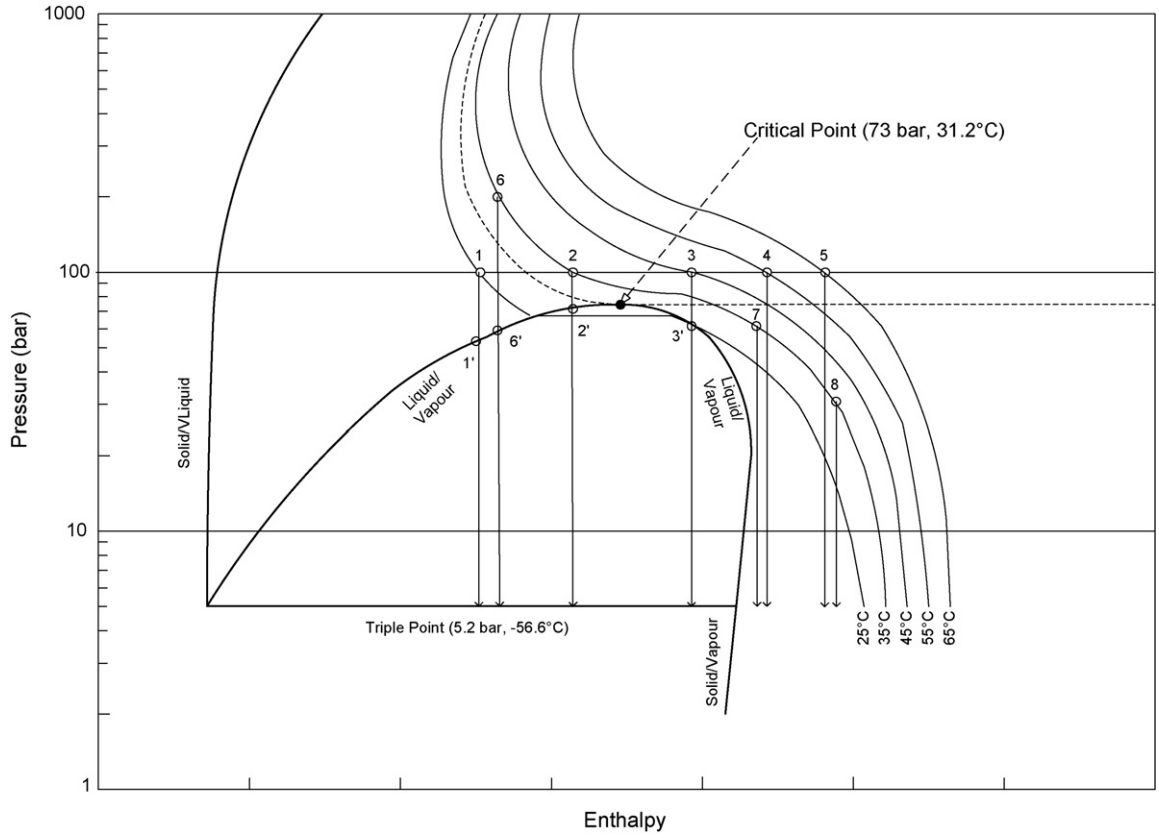


Fig. 4. Schematic diagram of the pressure–enthalpy of carbon dioxide (referenced from http://www.chemicalogic.com). The points corresponding to each initial pressure and temperature were labeled by unfilled circle. Thin solid line indicated the temperature. Critical point was labeled as a black filled circle. The region above the dished line indicated supercritical fluid. Thick solid lines indicated the solid/liquid, solid/gas, liquid/gas and triple point, respectively.

theoretical results (see Fig. 5(a)). For 500 psi initial pressure, the data fit well with the adiabatic theoretical results. Significant heat transfer does not occur during the 1 s of discharge. For 1000 psi initial pressure, the data is better represented by the isothermal assumption. Heat transfer is more significant during the 2 s of discharge. For the 1500 and 3000 psi initial pressures, the experimental results are not between the theoretical results of adiabatic and isothermal models (see Fig. 5(b)). At these conditions $CO_2$ exhibits both gas and liquid behavior, and the theoretical models based on ideal gas assumption are no longer suitable. In addition, the experimental results have obviously two-stage decompression crossing the region of liquid/gas saturation curve. The exponential form of the theoretical model did not fit well with these cases although the model worked well for the gasses of air, hydrogen and nitrogen [2,3].

### 3.5. Oil extraction aided with explosion process

The total oil of 10 g canola flake was 4.17 g determined by overnight Soxhlet extraction using hexane. The cumulative curve of supercritical $CO_2$ extraction had convective-controlled, transition, and diffusion-controlled extraction rate periods (Fig. 6). For the unexploded canola flake, the constant extraction rate period, defined by the linear equilibrium relationship between solute and solvent, occurred during the first 3 h until about 43% of the available oil was removed. After this period, the extraction rate slowly decreased and eventually entered into a diffusion-controlled period after 7 h when almost 63% of the oil was extracted. The mode of extraction curve was similar to that obtained by Przybylski et al. [16] under the extraction conditions, 6000 psi, 40 °C and 10 l/min flow rate, but the total extracted oil was lower probably because of lower flow rates in this experiment. However, it was comparable to that obtained under similar extraction conditions of 4931 psi and 40 °C [17].

For the exploded canola flake, the extraction curve was lower than that of unexploded canola flake during the first 3 h extraction, but the extraction curve for the exploded canola flake was higher than that of unexploded canola flake during the later 4 h extraction. It seems that the explosion process extended the constant extraction rate period and might improve solubility extraction of oil, resulting in more extracted oil.

The canola flake from a commercial crushing plant was processed with preheating, flaking and cooking. To some extent, the cell wall of canola seed may have been disrupted and the minute lipid particles coalesced to form large oil droplets, partially moving onto the surface [18]. The ruptured oil was normally easily extracted during the constant extraction rate period. However, the explosion process may have affected this coalesced oil in this experiment, which may explain the phenomena of the lower oil extraction during the first 3 h after explosion treatment. One possibility was due to the effect of oil loss in the explosion process. The oil dissolved in $CO_2$ at different initial explosion

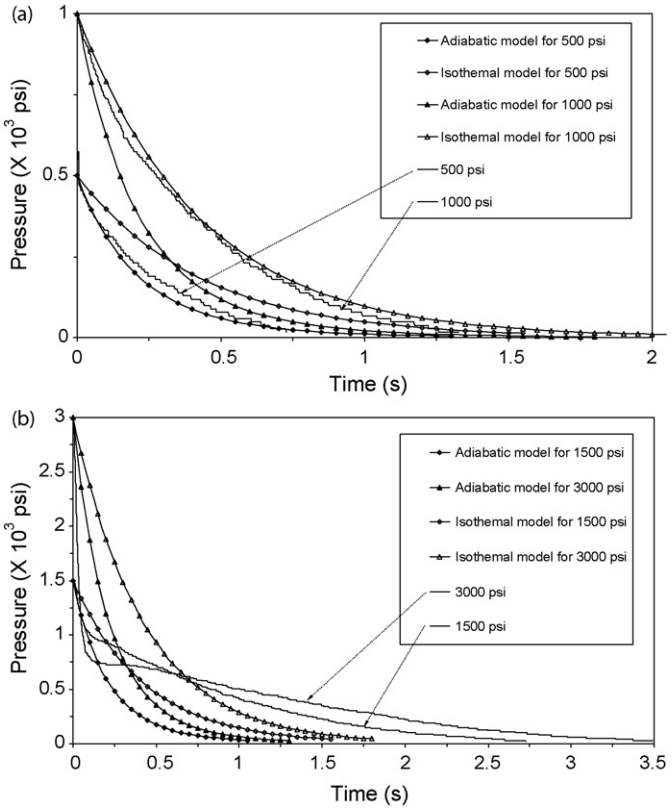


Fig. 5. Theoretical and experimental curves of explosion process for Case C with (a) 500 and 1000 psi initial pressure and (b) 1500 and 3000 psi initial pressures.

conditions was released with the high-pressure $CO_2$. For example, at 35 °C and 1500 psi, the oil solubility of canola oil was about 0.5 mg/g $CO_2$ and the density of $CO_2$ was 0.65 g/cm$^3$ [19]. It was estimated that 16 mg oil might have been released during the explosion process in this experiment. Another possibility was that the explosion process broke the coalesced oil droplets and disrupted the mixture of oil and solid matrix of canola flake, making this normally easily extracted oil more difficult to extract if oil was first absorbed back into the substrate.

The reduced oil extracted in the first 3 h may result in more oil extracted in the following 4 h, which could conceal both positive or negative effect of explosion on extractability.

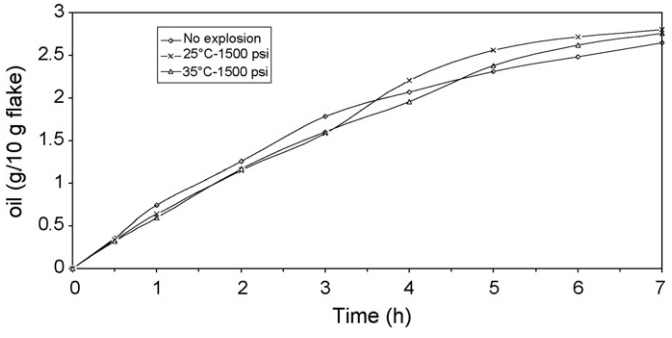


Fig. 6. Cumulative extraction curve following explosion process. *Note*: Data were the oil yields based on single extraction. Extraction conditions: 5000 psi, 50 °C and 700 ml/min flow rate.

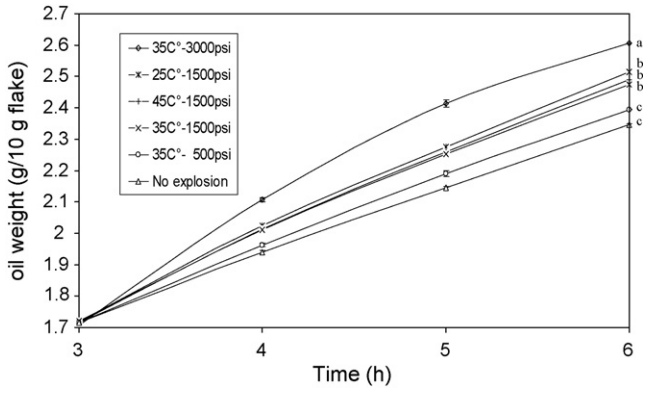


Fig. 7. Cumulative extraction curve following intermittent explosion after 3 h of initial extraction. Extraction conditions: 5000 psi, 50 °C and 700 ml/min flow rate. Different letters show significant difference using LSD test ($\alpha < 0.05$) for cumulative extraction yield after 3 h.

To minimize the effect of oil loss and the disruption of the coalesced oil from explosion, the process was integrated after the surface oil was extracted in the first 3 h and followed by another 3 h of extraction. The explosion process was expected to improve solubility-controlled extraction. The cumulative extraction curve for the later 3 h is shown in Fig. 7. The results showed that all explosion processes improved the oil extractability with higher yields during the later 3 h extraction, except for the 500 psi initial pressure at 35 °C condition, most likely due to low initial pressure. At a pressure of 1500 psi, extraction at temperatures of 25, 35 and 45 °C did not result in significantly different yields. However, the yield at lower temperature of 25 °C was comparable to 35 and 45 °C. This interesting result might show the cryogenic effect was more pronounced than a penetration-improved effect of higher temperature of 45 °C. At the temperature of 35 °C, increasing pressures of 500, 1500 and 3000 psi resulted in the obviously higher oil yields. The highest yield was achieved at initial condition of 35 °C and 3000 psi.

For the effect of temperature and pressure in the different range on enzyme hydrolysis of pretreated lignocelluloses, both consistent and contentious results appeared in different studies [9,10]. Higher glucose yields were associated with the higher temperatures and pressures of explosion for cellulose hydrolysis [9]. However, a higher glucose yield was obtained at a lower explosion pressure of 3100 psi compared to 4000 psi at the same temperature of 165 °C for lignocellulosic hydrolysis [10]. Other factors such as original anatomical structure, moisture content of sample and pretreatment time contributed to the results of pretreatment [9,10,13]. The results for the effect of temperature and pressure might be interpreted from other multiple factors. The canola flake is a very oily material and should have its own explosion characteristics compared to other non- or low-oil materials. As noted in the methods, canola flake was frozen overnight after explosion. The effect on the cell structure was not measured in this study, but with 4% moisture, the freezing effect of water during storage was expected to be very little in comparison to the potential effect of saturated $CO_2$ during the explosion process where rapidly falling temperatures occur during $CO_2$ expansion.

The fatty acid composition of oil for the percentages of the main components, C16:0, C18:0, C18:1, C18:2, C18:3 and C20:0 showed no significant difference compared to oil extracted from unexploded flake according to Dunnett's test at 95% confidence determined by SAS.

## 4. Conclusion

The mechanism of high-pressure explosion for many biological applications is still not clear. Initial pressure and temperature, which determine the phase and property of $CO_2$, were chief parameters. By combining the engineering and biological viewpoints, the present study discussed phase transition and temperature change associated with pressure–time history during the explosion process. The results are important to gain understanding of the mechanism or to direct further experimental design and analysis.

The theoretical model of depressurization under the isentropic assumptions for ideal gas worked for $CO_2$ in sub-critical conditions, but did not fit the experimental results for supercritical $CO_2$, especially when two-stage decompression occurred. A new model is required to represent the property of gas and phase change under different initial conditions.

The improvement of oil extractability through high-pressure $CO_2$ explosion treatment was demonstrated using canola flake as a biological model system. The explosion at an initial condition of 35 °C and 3000 psi resulted in the highest oil yield after supercritical $CO_2$ extraction. Different explosion conditions did not affect the fatty acid composition of the oil. The potential application of this explosion process for other materials need to be further investigated. For example, if the explosion process could alternate the cooking process and achieve the purposes to improve oil extractability, and deactivate the enzyme myrosinase at the same time. Then uncooked canola flake could be directly used for supercritical $CO_2$ extraction.

## Acknowledgements

Southern Regional Canola Research Program of the US Canola Association funded research work. Archer Daniels Midland Company (ADM) donated canola flake sample. We also acknowledge Dr. Susan Duckett for help with lipid analysis.

## References

[1] W.R. Byrnes, R.C. Reid, F.E. Ruccia, Rapid depressurization of a gas storage cylinder, I&EC Process Des. Dev. 3 (1964) 206–209.
[2] A.L. Addy, B.J. Walker, Rapid discharging of a vessel through a nozzle or an orifice, ASME (1972) 1–8, 72-FE-40.
[3] J.C. Dutton, R.E. Coverdill, Experiments to study the gaseous discharge and filling of vessels, Int. J. Eng. Educ. 13 (1997) 123–134.
[4] J. Zhang, T.A. Davis, M.A. Matthews, M.J. Drews, M. LaBerge, Y.H. An, Sterilization using high-pressure carbon dioxide—a review, J. Supercrit. Fluid 38 (3) (2006) 354–372.
[5] A. White, D. Burns, T.W. Christensen, Effective terminal sterilization using supercritical carbon dioxide, J. Biotechnol. 123 (2006) 504–515.
[6] S. Spilimbergo, N. Elvassore, A. Bertucco, Microbial inactivation by high-pressure, J. Supercrit. Fluid 22 (2002) 55–63.
[7] C. Bauer, D. Steinberger, G. Schlauer, T. Gamse, R. Marr, Activation and denaturation of hydrolases in dry and humid supercritical carbon dioxide, J. Supercrit. Fluid 19 (2000) 79–86.
[8] N.T. Dunford, F. Temelli, Effect of supercritical $CO_2$ on myrosinase activity and glucosinolate degradation in canola, J. Agric. Food Chem. 44 (1996) 2372–2376.
[9] Y. Zheng, H.M. Lin, G.T. Tsao, Supercritical carbon dioxide explosion as a pretreatment for cellulose hydrolysis, Biotechnol. Prog. 17 (1998) 890–896.
[10] K.H. Kim, J. Hong, Supercritical $CO_2$ pretreatment of lignocellulose enhances enzymatic cellulose hydrolysis, Bioresour. Technol. 77 (2001) 139–144.
[11] W.W. Christie, A simple procedure for rapid transmethylation of glycerolipids and cholesteryl esters, J. Lipid Res. 23 (1982) 1072–1076.
[12] R.V. Shende, T.R. Redfearn, S.J. Lombardo, Defect formation during supercritical extraction of binder from green ceramic components, J. Am. Ceram. Soc. 87 (2004) 1254–1258.
[13] F. Gaspar, R. Santos, M.B. King, Disruption of glandular trichomes with compressed $CO_2$: alternative matrix pre-treatment for $CO_2$ extraction of essential oils, J. Supercrit. Fluid 21 (2001) 11–12.
[14] F. Jaouad, S. Anand, Process for preparing materials for extraction, International Patent WO 2,006,047,445 (2006).
[15] M.A. Saad, Compressible Fluid Flow, 2nd ed., Prentice-Hall, Englewood Cliffs, NJ, 1993, pp. 103–109.
[16] R. Przybylski, Y. Lee, I. Kim, Oxidative stability of canola oils extracted with supercritical carbon dioxide, Lebensmitt. Wiss. u. Technol. 31 (1998) 687–693.
[17] E. Jenab, K. Rezaei, Z. Emam-Djomeh, Canola oil extracted by supercritical carbon dioxide and a commercial organic solvent, Eur. J. Lipid Sci. Technol. 108 (2006) 488–492.
[18] E.H. Unger, Commercial processing of canola and rapeseed: crushing and oil extraction, in: F. Shahidi (Ed.), Canola and Rapeseed Production: Chemistry, Nutrition, and Processing Technology, Van Nostrand Reinhod, New York, 1990.
[19] M. Fattori, N.R. Bulley, A. Meisen, Carbon dioxide extraction of canola seed: oil solubility and effect of seed treatment, J. Am. Oil Chem. Soc. 65 (6) (1988) 968–974.